Heterogeneous Catalysis

DOI: 10.1002/anie.201004966

High Activity of $Ce_{1-x}Ni_xO_{2-y}$ for H_2 Production through Ethanol Steam Reforming: Tuning Catalytic Performance through Metal–Oxide Interactions**

*Gong Zhou, Laura Barrio, Stefano Agnoli, Sanjaya D. Senanayake, Jaime Evans, Anna Kubacka, Michael Estrella, Jonathan C. Hanson, Arturo Martínez-Arias, Marcos Fernández-García, and José A. Rodriguez**

Hydrogen production by the steam reforming of ethanol ($C_2H_5OH + 3H_2O \rightarrow 6H_2 + 2CO_2$) is receiving significant attention because ethanol can be obtained readily from renewable-energy sources and is environmentally friendly.[1–3] There is also a strong interest in the use of ethanol as a fuel for mobile-fuel-cell applications.[4,5] The ethanol-reforming process occurs by a complex mechanism involving multiple reactions.[2,6] Noble-metal supported catalysts, in particular Rh, have been shown to have significant activity;[3,6–10] however, the high cost of these materials limits their applications. As a less expensive alternative, highly active[3,11–15] nickel-based catalysts have been studied for the production of H_2 through ethanol steam reforming.[16–18] These catalysts readily undergo deactivation as a result of coke deposition.[17,18] Herein, we describe a successful approach to the production of highly efficient, stable, and inexpensive nickel-based catalysts for ethanol steam reforming. Within the $Ce_{1-x}Ni_xO_{2-y}$ system, metal–oxide interactions alter the chemical properties of nickel and ceria to produce surface sites which are very active for the cleavage of C–C and C–H bonds and for the subsequent formation of CO_2 and H_2.

Recently, the structural and electronic properties of $Ce_{1-x}Ni_xO_{2-y}$ nanosystems prepared by a reverse-microemulsion method were characterized by synchrotron-based X-ray diffraction (XRD), X-ray absorption fine structure (XAFS), Raman spectroscopy, and density-functional calculations.[19] XRD showed that the solubility limit of a Ce–Ni exchange in ceria is in the range of 10–12%. In a $Ce_{0.9}Ni_{0.1}O_{2-y}$ system, most of the Ni forms a solid solution, whereas in a sample with higher Ni content (20%), there is also a segregated phase of NiO present.[19] Results of in situ time-resolved XRD indicate that strong Ce–O–Ni interactions in the mixed-metal oxide delay the reduction of the nickel cations by hydrogen up to temperatures above 400 °C. Hydrogen reduction of the $Ce_{1-x}Ni_xO_{2-y}$ mixed-metal oxides involves the reduction of Ce^{IV} species to Ce^{III}, as well as Ni^0 formation.[19]

During the steam reforming of ethanol on a $Ce_{0.8}Ni_{0.2}O_{2-y}$ catalyst, substantial evolution of H_2 and CO_2 was observed at temperatures above 300 °C (Figure 1). The variations in the H_2 and CO_2 signals track each other, as expected for a catalytic process. Ni is a well-known methanation catalyst.[20] In the experiments with $Ce_{0.8}Ni_{0.2}O_{2-y}$, the amount of methane formed was either very small (300–400 °C) or negligible (400–

[*] Dr. G. Zhou, Dr. L. Barrio, Dr. S. Agnoli, Dr. S. D. Senanayake, M. Estrella, Dr. J. C. Hanson, Dr. J. A. Rodriguez
Chemistry Department, Brookhaven National Laboratory
Upton, NY 11973 (USA)
Fax: (+1) 631-344-5815
E-mail: rodrigez@bnl.gov
Prof. J. Evans
Facultad de Ciencias, Universidad Central de Venezuela
Caracas 1020 A (Venezuela)
Dr. A. Kubacka, Dr. A. Martínez-Arias, Dr. M. Fernández-García
Instituto de Catálisis y Petroleoquímica, CSIC
Campus Cantoblanco, 28049 Madrid (Spain)

[**] The research at BNL was financed by the US Department of Energy (DOE), Chemical Sciences Division, Office of Basic Energy Science (DE-AC02-98CH10086). The National Synchrotron Light Source is supported by the Divisions of Materials and Chemical Sciences of the US DOE. L.B. acknowledges funding by the FP7 People program under the project Marie Curie IOF-219674. J.E. thanks INTEVEP and IDB for research grants that made possible part of this research at the Universidad Central de Venezuela. Research at the ICP-CSIC was financed by the Comunidad de Madrid (DIVERCEL S2009/ENE-1745) and the MICINN (CTQ2006-15600/BQU and CTQ2009-14527/BQU), to whom we are grateful.

Supporting information for this article is available on the WWW under http://dx.doi.org/10.1002/anie.201004966.

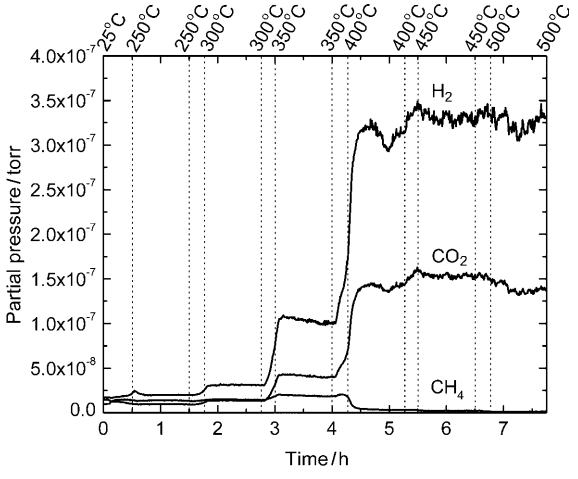

Figure 1. Production of H_2, CO_2, and CH_4 during the steam reforming of ethanol over a $Ce_{0.8}Ni_{0.2}O_{2-y}$ catalyst. The sample was held under isothermal conditions at 250, 300, 350, 400, 450, and 500 °C for periods of 1 h. The amount of H_2, CO_2, and CH_4 was measured with a mass spectrometer located at the exit of the microreactor.[19] The measured values are reported without correction for the relative sensitivities of H_2, CO_2, and CH_4 in the mass spectrometer.

500 °C). This behavior is very different from that observed for the steam reforming of ethanol on other NiO/CeO_2 catalysts,[16–18] with which a significant amount of methane was formed, with eventual deactivation owing to coke deposition. We tested the catalytic activity of $Ce_{0.8}Ni_{0.2}O_{2-y}$ for long periods (10–40 h) at 400–500 °C and always observed the stable production of H_2 and CO_2 (see Figure S1 in the Supporting Information). Metal–oxide interactions give the nickel present in $Ce_{0.8}Ni_{0.2}O_{2-y}$ special chemical properties.

We examined the production of hydrogen by the steam reforming of ethanol in a temperature range between 250 and 500 °C over CeO_2, Rh/CeO_2, $Ce_{1-x}Ni_xO_{2-y}$, and Ni/CeO_2 catalysts (Figure 2). The pure ceria support was not active for the ethanol-steam-reforming reaction and produced a negligible amount of hydrogen even at 500 °C. With both $Ce_{0.9}Ni_{0.1}O_{2-y}$ and $Ce_{0.8}Ni_{0.2}O_{2-y}$, a small amount of H_2 was produced as soon as the temperature was raised to 300 °C. At temperatures below 400 °C, the reforming activities of both mixed oxides were nearly identical. However, for $Ce_{0.8}Ni_{0.2}O_{2-y}$, substantial catalytic activity was observed at

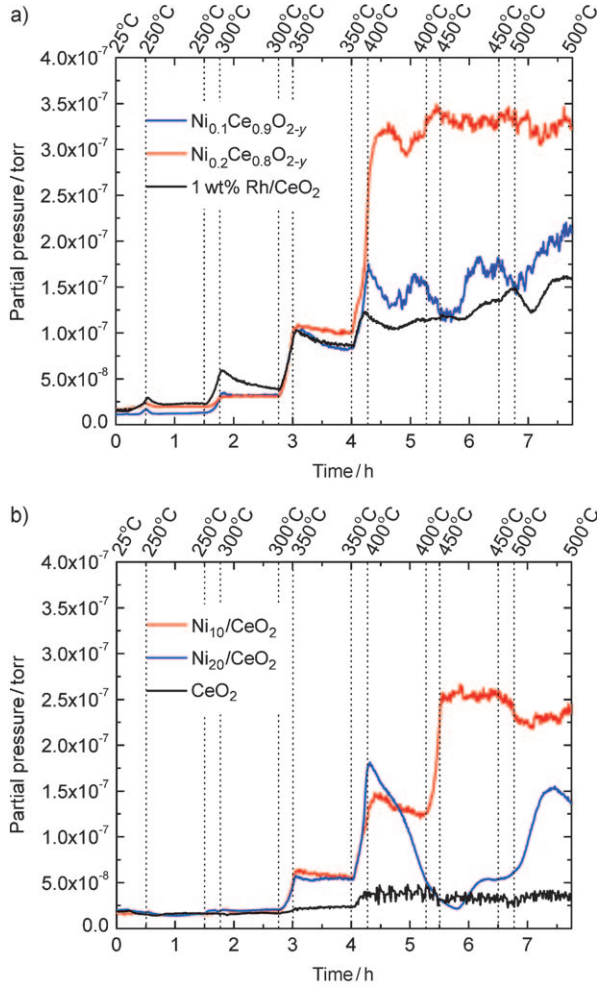

Figure 2. a) Hydrogen-production plots for ethanol steam reforming over $Ni_{0.1}Ce_{0.9}O_{2-y}$, $Ni_{0.2}Ce_{0.8}O_{2-y}$, and 1 wt% Rh/CeO_2. b) Hydrogen-production plots for ethanol steam reforming over Ni_{10}/CeO_2, Ni_{20}/CeO_2, and CeO_2. The samples were held under isothermal conditions at 250, 300, 350, 400, 450, and 500 °C for periods of 1 h.

400 °C; this activity was very stable over time (see also Figure S1 in the Supporting Information). Hydrogen production with $Ce_{0.8}Ni_{0.2}O_{2-y}$ was almost twice that observed for $Ce_{0.9}Ni_{0.1}O_{2-y}$. Between 400 and 500 °C, the reforming activities of both mixed oxides were relatively stable and only increased slightly. The estimated ethanol consumption of $Ni_{0.2}Ce_{0.8}O_{2-y}$ at 400 °C was 100 %, and the selectivity for H_2 formation was 67 %. The production of hydrogen over a typical Rh/CeO_2 catalyst is described in Figure 2a. At low temperatures (< 300 °C), the activity of Rh/CeO_2 was higher than that of the mixed-metal oxides, but at high temperatures (> 400 °C), the performance of the $Ce_{1-x}Ni_xO_{2-y}$ systems was far superior. Clearly, $Ce_{0.8}Ni_{0.2}O_{2-y}$ is a nonexpensive highly efficient catalyst for ethanol steam reforming.

The data in Figure 2b for the nickel-impregnated samples Ni_{10}/CeO_2 and Ni_{20}/CeO_2 (10 and 20 mol % Ni deposited on the ceria support) show that hydrogen production started at a temperature of 350 °C. Ni_{10}/CeO_2 showed the highest activity at 450 °C; its hydrogen production decreased slightly as the temperature was raised to 500 °C. On the other hand, Ni_{20}/CeO_2 became catalytically unstable at temperatures above 400 °C, with rapid deactivation. When the temperature was raised to 450 and 500 °C, Ni_{20}/CeO_2 regained some activity, but its hydrogen production was unstable. The deactivation of Ni_{20}/CeO_2 is probably due to metal-particle sintering and coke deposition.[16–18] The two best catalysts studied are $Ce_{0.8}Ni_{0.2}O_{2-y}$ and Ni_{10}/CeO_2, whereby the mixed-metal oxide displays the highest activity for H_2 production.

The catalysts described in Figure 2 were characterized by XAFS spectroscopy and XRD (see Figure S2 and S3 in the Supporting Information). An analysis of the Ni K-edge XAFS region showed that nickel in the as-prepared catalysts was in a +2 oxidation state. In their XRD data, all samples showed a major contribution from a CeO_2 fluorite-type structure.[21] The lattice parameters of the fresh catalysts were nearly identical at 5.417 Å, and very close to the reported value for bulk ceria of 5.411 Å.[21] The $Ce_{0.9}Ni_{0.1}O_{2-y}$ sample appeared to be a single-phase solid solution and did not exhibit any clear peaks associated with the NiO phase.[19] The diffraction patterns of $Ce_{0.8}Ni_{0.2}O_{2-y}$ (Figure 3), Ni_{10}/CeO_2, and Ni_{20}/CeO_2 samples exhibited weak NiO peaks that indicated the presence of an NiO phase in these systems. The XRD Rietveld refinements gave NiO mole fractions for $Ce_{0.8}Ni_{0.2}O_{2-y}$, Ni_{10}/CeO_2, and Ni_{20}/CeO_2 of 0.11, 0.1, and 0.18, respectively. The XRD results suggest that for $Ce_{0.8}Ni_{0.2}O_{2-y}$, only about half of the Ni atoms present in the sample form a periodic structure of NiO. The rest of the Ni atoms form a solid solution in the ceria lattice.[19]

Figure 3 shows a series of XRD patterns for $Ce_{0.8}Ni_{0.2}O_{2-y}$ collected during the steam reforming of ethanol. The diffraction signal is governed by ceria contributions, with weak features for NiO. Rietveld refinement revealed that under the reaction conditions, NiO survives up to about 400 °C, at which temperature a NiO→Ni transformation takes place. The appearance of the metallic Ni phase correlated with a substantial increase in the production of H_2 (Figure 1). Thus, the best catalyst in Figure 2 contains a small amount of Ni (particles less than 3 nm in diameter) dispersed on a nickel-doped ceria support. In the case of $Ce_{0.9}Ni_{0.1}O_{2-y}$, which

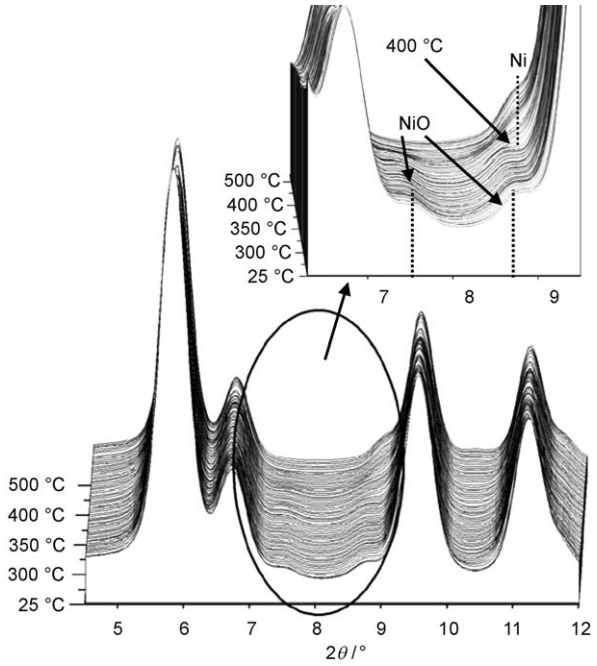

Figure 3. Time-resolved X-ray diffraction patterns for $Ce_{0.8}Ni_{0.2}O_{2-y}$ collected during the ethanol-steam-reforming reaction. The graph at the top is an expanded view of the bottom graph in the 2θ range 6.5–9.5°; the dotted lines show the positions of the NiO and Ni peaks.

was not as active as $Ce_{0.8}Ni_{0.2}O_{2-y}$, no significant amounts of Ni were detected by XRD under the reaction conditions (see Figure S4 in the Supporting Information).

A comparison of the XRD data for $Ce_{0.8}Ni_{0.2}O_{2-y}$ and Ni_{10}/CeO_2 illustrates the important role played by the oxide support in the catalytic process. Initially, the mole fractions of NiO in these systems were very close (ca. 0.1), and high catalytic activity was observed following an NiO→Ni transformation at temperatures above 400 °C. Thus, differences in the catalytic activity of these systems (Figure 2) reflect variations in the properties of the oxide component that may directly affect the reaction process or metal–oxide interactions. Rietveld refinement of the in situ XRD patterns showed that for both catalysts there was a large expansion of the oxide lattice cell at temperatures between 200 and 250 °C (Figure 4). Ni_{10}/CeO_2 exhibited a lattice expansion very close to that found in similar experiments with pure CeO_2. Upon thermal treatment, an expansion of the lattice is expected; however, sudden changes in the slope can be related to chemical processes and particularly to the creation of O vacancies and Ce^{III} sites, which have larger atomic radii than Ce^{IV} sites.[22,23] It is known that ceria surfaces undergo significant reduction upon reaction with ethanol.[24,25] The cell expansion in $Ce_{0.8}Ni_{0.2}O_{2-y}$ is 1.5 times larger than in Ni_{10}/CeO_2, which indicates that the number of O vacancies is substantially larger in the mixed-metal oxide. The doping of ceria with Ni induces strain in the oxide lattice and favors the formation of O vacancies.[19] A large concentration of O vacancies, and related defects, should enhance the dispersion of reduced Ni on the oxide surface[26] and facilitate the cleavage of the O–H bonds in water and ethanol.[22–25]

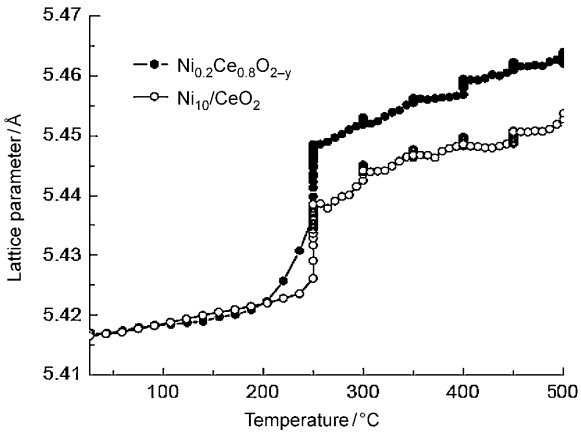

Figure 4. Sequential Rietveld refinement analysis of the ceria lattice parameter for $Ce_{0.8}Ni_{0.2}O_{2-y}$ and Ni_{10}/CeO_2 catalysts under ethanol steam reforming at different temperatures.

The data for Ni_{10}/CeO_2 and Ni_{20}/CeO_2 in Figure 2 indicate that the Ni coverage has a drastic effect on the catalytic activity. Figure 5 shows valence photoemission spectra recorded after Ni had been deposited at submonolayer coverage on a $CeO_2(111)$ film grown on Ru(0001) according to a previously described procedure.[26,27] Clean $CeO_2(111)$ is characterized by a large band gap, with the O 2p states appearing at binding energies between 3 and 8 eV.[27] The addition of small amounts of nickel (< 0.4 monolayer) produces new features at binding energies between 0 and 2 eV, in the region in which the Ni 3d states are expected.[28,29] A detailed comparison of the valence spectra for Ni/CeO_2 and bulk Ni[28,29] shows that metal–oxide interactions significantly

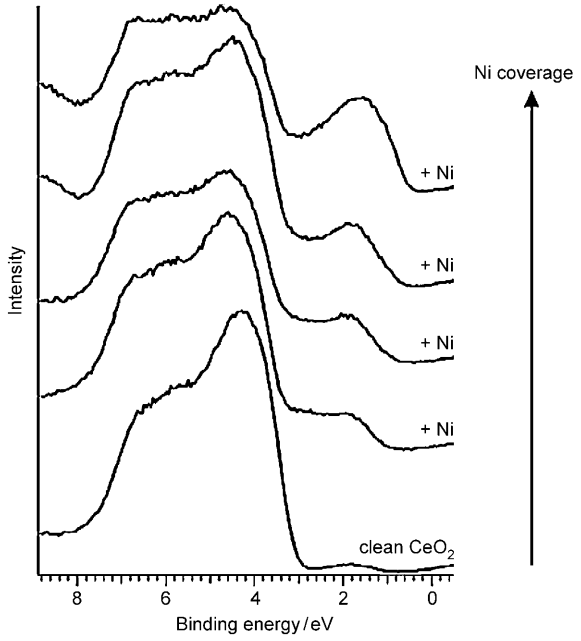

Figure 5. Valence photoemission spectra (He II radiation; 40.8 eV) for the deposition of small amounts of Ni (< 0.4 monolayer) on a $CeO_2(111)$ surface.

decrease the density of occupied Ni 3d states near the Fermi level.

The smaller the Ni coverage, the larger the electronic perturbations of Ni: at the smallest Ni coverage in Figure 5, Ni 2p X-ray photoelectron spectra (see Figure S5 in the Supporting Information) showed the dominant presence of Ni^{2+} on the oxide surface. An electronically perturbed Ni^0 species becomes the dominant species for the other nickel coverages. The electronic perturbations of nickel modify its chemical properties and thus decrease its activity for the generation of methane. Figure 6 shows the CO-methanation

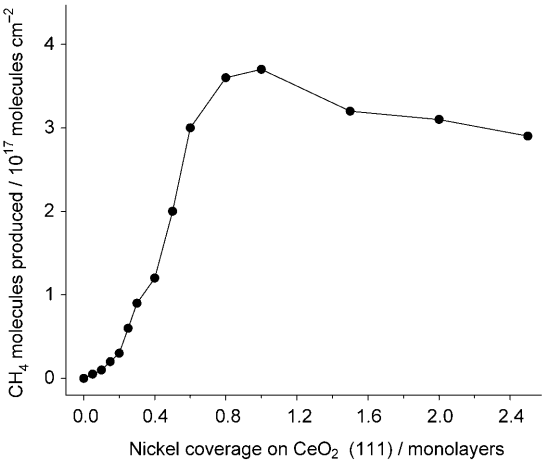

Figure 6. CO-methanation activity of model $Ni/CeO_2(111)$ catalysts as a function of admetal coverage. Each $Ni/CeO_2(111)$ surface was exposed to a mixture of CO (24 torr) and H_2 (96 torr) at approximately 350 °C. The reported values correspond to the number of CH_4 molecules produced per square centimeter of the catalyst surface during a reaction time of 5 min under steady-state conditions.

activity of $Ni/CeO_2(111)$ surfaces as a function of nickel coverage. This reaction is a major source of CH_4 in the ethanol-steam-reforming process.[6] At large coverages of Ni, the $Ni/CeO_2(111)$ systems exhibit comparable methanation activity to that of bulk-nickel surfaces.[20,30] In contrast, at low coverages (< 0.4 monolayer) of Ni, the amount of methane produced is very small or negligible. These $Ni/CeO_2(111)$ systems with a low nickel content were transformed into $Ni/CeO_{2-x}(111)$ during the reaction. They displayed a high activity/selectivity for ethanol steam reforming and did not undergo deactivation with time. In this respect, their behavior is similar to that found for the powder Ni_{10}/CeO_2 catalyst, which did not show signs of deactivation after a reaction time of 40 h.

In summary, $Ce_{0.8}Ni_{0.2}O_{2-y}$ is an excellent catalyst for ethanol steam reforming. It is less expensive than Rh/CeO_2 and has a higher catalytic activity. Under the reaction conditions, $Ce_{0.8}Ni_{0.2}O_{2-y}$ contains small particles of nickel dispersed on partially reduced nickel-doped ceria. Metal–oxide interactions perturb the electronic properties of Ni and suppress its activity for methanation; at the same time, the nickel embedded in ceria induces the formation of O vacancies that facilitate the cleavage of the O–H bonds in ethanol and water. These studies show the importance of both the metal and the oxide phase in catalysts for ethanol steam reforming. Both phases must be taken into consideration when trying to improve catalyst performance.

Experimental Section

The $Ni_{0.1}Ce_{0.9}O_{2-y}$ and $Ni_{0.2}Ce_{0.8}O_{2-y}$ catalysts were prepared by the use of reverse microemulsions.[19] Ni K-edge XAFS spectra were collected in air at room temperature on beamline X18A of the National Synchrotron Light Source (NSLS) at Brookhaven National Laboratory.[19] In situ time-resolved XRD experiments were carried out on beamline X7B of the NSLS ($\lambda = 0.3184$ Å). The sample (ca. 5 mg) was loaded into a glass capillary cell, which was attached to a flow system.[19,22] A small resistance heater was wrapped around the capillary, and the temperature was monitored with a 1.0 mm Chromel–Alumel thermocouple, which was placed directly in the capillary near the sample. Two-dimensional powder patterns were collected with an Mar345 image-plate detector, and the powder rings were integrated by using the FIT2D code.[31] The short wavelength enabled powder-profile refinement of data to $q = 10$ $Å^{-1}$ Lattice constants were determined by Rietveld analysis with the General Structure Analysis System (GSAS) program.[32,33] Diffraction patterns were collected over the catalysts during ethanol steam reforming. The reaction was carried out isothermally at several temperatures (250, 300, 350, 400, 450, and 500 °C) with He as the carrier gas. The He flow rate to the reactor was maintained at 10 mL min^{-1}. A vapor mixture of water and ethanol (6:1) was injected into the gas stream by using a syringe pump at a vapor flow rate of 0.532 mL min^{-1}. The reaction products were identified with a quadrupole mass spectrometer.

The experiments with $Ni/CeO_2(111)$ surfaces were undertaken in two different ultrahigh-vacuum (UHV) chambers.[34,35] One of the chambers was used to collect the XPS ($Mg_{K\alpha}$) and valence photoemission spectra (He II) data. To avoid problems with charging in the photoemission experiments, films of $CeO_2(111)$ were grown in situ on Ru(0001).[26,27] Studies of CO methanation and ethanol steam reforming on $Ni/CeO_2(111)$ were conducted in a second UHV chamber with a batch reactor attached.[34,35] The kinetic tests were carried out by using a $CeO_2(111)$ single crystal cleaned by standard procedures.[35] After preparation and characterization of the $Ni/CeO_2(111)$ surfaces by vapor-deposition of Ni on the oxide substrate, the sample was transferred to the reactor. The reported rates are for steady-state conditions. The amount of hydrogen produced was normalized according to the exposed active area of the sample face that contained nickel.[35]

Received: August 9, 2010
Published online: November 9, 2010

Keywords: ceria · ethanol · hydrogen production · nickel · steam reforming

[1] A. Demirbas, *Prog. Energy Combust. Sci.* **2007**, *33*, 1–18.
[2] M. Ni, D. Y. C. Leung, M. K. H. Leung, *Int. J. Hydrogen Energy* **2007**, *32*, 3238–3247.
[3] A. Haryanto, S. Fernando, N. Murali, S. Adhikari, *Energy Fuels* **2005**, *19*, 2098–2106.
[4] P. D. Vaidya, A. E. Rodrigues, *Chem. Eng. J.* **2006**, *117*, 39–49.
[5] L. E. Arteaga, L. Peralta, V. Kafarov, Y. Casas, E. Gonzales, *Chem. Eng. J.* **2008**, *136*, 256–266.
[6] H. Idriss, *Platinum Met. Rev.* **2004**, *48*, 105–115.
[7] M. Scott, M. Goeffroy, W. Chiu, M. A. Blackford, H. Idriss, *Top. Catal.* **2008**, *51*, 13–21.
[8] A. Erdohelyi, J. Raskó, T. Kecskés, M. Tóth, M. Dömök, K. Baán, *Catal. Today* **2006**, *116*, 367–376.

[9] J. R. Salge, G. A. Deluga, L. D. Schmidt, *J. Catal.* **2005**, *235*, 69 – 78.
[10] J. Kugai, S. Velu, C. Song, *Catal. Lett.* **2005**, *101*, 255 – 264.
[11] J. Beckers, C. Gaudillère, D. Farrusseng, G. Rothenberg, *Green Chem.* **2009**, *11*, 921 – 925.
[12] V. M. Gonzalez-De la Cruz, J. P. Holgado, R. Pereñíguez, A. Caballero, *J. Catal.* **2008**, *257*, 307 – 314.
[13] F. Auprêtre, C. Descorme, D. Duprez, *Catal. Commun.* **2002**, *3*, 263 – 267.
[14] A. N. Fatsikostas, X. E. Verykios, *J. Catal.* **2004**, *225*, 439 – 452.
[15] J. Comas, F. Mariño, M. Laborde, N. Amadeo, *Chem. Eng. J.* **2004**, *98*, 61 – 68.
[16] F. Romero-Sarria, J. C. Vargas, A.-C. Roger, A. Kiennemann, *Catal. Today* **2008**, *133*, 149 – 153.
[17] H. Fajardo, L. Probst, N. Carreño, I. Garcia, A. Valentini, *Catal. Lett.* **2007**, *119*, 228 – 236.
[18] L. Jalowiecki-Duhamel, C. Pirez, M. Capron, F. Dumeignil, E. Payen, *Catal. Today* **2010**, *157*, 456 – 461 .
[19] L. Barrio, A. Kubacka, G. Zhou, M. Estrella, A. Martínez-Arias, J. C. Hanson, M. Fernández-García, J. A. Rodriguez, *J. Phys. Chem. C* **2010**, *114*, 12689 – 12697.
[20] R. D. Kelley, D. W. Goodman, *Surf. Sci.* **1982**, *123*, L743 – L749.
[21] PDF 340394, *JCPDS Powder Diffraction File*, International Center for Diffraction Data, Swathmore, PA, **1998**.
[22] X. Q. Wang, J. A. Rodriguez, J. C. Hanson, D. Gamarra, A. Martínez-Arias, M. Fernández-García, *Top. Catal.* **2008**, *49*, 7 – 15.
[23] X. Q. Wang, J. C. Hanson, G. Liu, J. A. Rodriguez, A. Iglesias-Juez, M. Fernández-García, *J. Chem. Phys.* **2004**, *121*, 5434 – 5444.
[24] P. Y. Sheng, W. W. Chiu, A. Yee, S. J. Morrison, H. Idriss, *Catal. Today* **2007**, *129*, 313 – 321.
[25] D. R. Mullins, S. D. Senanayake, T.-L. Chen, *J. Phys. Chem C* **2010**, *114*, 17112 – 17119.
[26] Y. Zhou, J. M. Perket, A. B. Crooks, J. Zhou, *J. Phys. Chem. Lett.* **2010**, *1*, 1447.
[27] D. R. Mullins, S. H. Overbury, D. R. Huntley, *Surf. Sci.* **1998**, *409*, 307 – 316.
[28] D. E. A. Gordon, R. M. Lambert, *Surf. Sci.* **1993**, *287/288*, 114 – 122.
[29] L. S. Cederbaum, W. Domcke, W. von Niessen, W. Brenig, *Z. Phys. B* **1975**, *21*, 381 – 388.
[30] J. A. Rodriguez, D. W. Goodman, *Surf. Sci. Rep.* **1991**, *14*, 1 – 108.
[31] A. P. Hammersley, S. O. Svensson, A. Thompson, *Nucl. Instrum. Methods Phys. Res. Sect. A* **1994**, *346*, 312 – 321.
[32] B. H. Toby, *J. Appl. Crystallogr.* **2001**, *34*, 210.
[33] A. C. Larson, R. B. Von Dreele, *Los Alamos National Laboratory Report LAUR* **2000**, 86 – 748.
[34] J. A. Rodriguez, J. Graciani, J. Evans, J. B. Park, F. Yang, D. Stacchiola, S. D. Senanayake, S. Ma, M. Pérez, P. Liu, J. F. Sanz, J. Hrbek, *Angew. Chem.* **2009**, *121*, 8191 – 8194; *Angew. Chem. Int. Ed.* **2009**, *48*, 8047 – 8050.
[35] J. A. Rodriguez, P. Liu, J. Hrbek, J. Evans, M. Pérez, *Angew. Chem.* **2007**, *119*, 1351 – 1354; *Angew. Chem. Int. Ed.* **2007**, *46*, 1329 – 1332.

